

# Monte-Carlo Simulations for Heating of Superdense Matter by Relativistic Electrons

A. OKABAYASHI<sup>1,2)</sup>, T. YABUCHI<sup>1,2,3)</sup>, H. HABARA<sup>1,2)</sup> and K. A. TANAKA<sup>1,2)</sup>

<sup>1)</sup>*Department of Electrical, Electronic, and Information Engineering, Graduate School of Engineering, Osaka University, 2-1, Yamada-oka, Suita, Osaka, 565-0871, Japan*

<sup>2)</sup>*Institute of Laser Engineering, Osaka University, 2-6, Yamada-oka, Suita, Osaka, 565-0871, Japan*

<sup>3)</sup>*Center for Energy Research, University of California, San Diego, 9500 Gilman Drive, # 0417, La Jolla, CA 92093-0417, USA*

(Received: 19 September 2008 / Accepted: 11 March 2009)

We studied energy deposition by high energy electrons on highly compressed core plasma for fast ignition in inertial confinement fusion research. At present, the propagation of extreme high electron current in high density plasma has not been well understood experimentally, so that we calculate a collection of energy depositions by a single particle at core plasma using an electromagnetic cascade Monte-Carlo simulation, EGS5, in order to estimate the distribution of temperature in the superdense matter. The construction of superdense matter and physical parameters were taken from a previous experiment. In the results, the temperature increases from the low dense plasma to core region and the maximum temperature is obtained at the core up to several tens eV.

Keywords: Monte-Carlo simulation, superdense matter, relativistic electrons, collisional process, energy deposition, core temperature

## 1. Introduction

In fast ignition [1](FI) in inertial confinement fusion research, many laser beams implode a spherical fuel shell to create a superdense plasma. Then, the ignition is induced by heating of the imploded core by fast electrons generated through ultra-intense laser-plasma interactions. Therefore, it is a key issue to know the interaction mechanism of ultra-intense laser light with long scale imploded plasma, and also energy deposition of fast electrons to the core plasma.

The energy of fast electrons for efficient heating is considered to range from hundreds of keV to several MeV at the core. In addition, high total energy is necessary to heat the core sufficiently to the ignition temperature. In the classical framework, physical processes are rather complicated when the electrons lose their energies via collisions in plasmas. In order to understand real phenomena in experiment one needs to take into account relativistic and collective effects on the propagation and deposition of fast electrons. From these reasons, at present the physical mechanisms have not been understood how high density electron current transports and deposits the energy in dense plasmas nevertheless a particle simulation predicts that binary collisions are relatively important at the core [2].

From these points of view, we carried out spatial temperature distribution in the superdense matter by the EGS5 (Electron Gamma Shower 5)[3] program based on the experimental parameters [4, 5, 6]. The result shows the energy range of electrons re-

sponsible for the energy deposition at a high density core plasma and also possible temperature increase expected through the collision by fast electrons.

EGS5 [3] is the electromagnetic cascade Monte-Carlo code of electron and photon transportation calculation in a wide-range of energies in an arbitrary geometry. Specifically, the transportation of electrons, photons, and positrons in any elements, compounds, and the mixture can be treated. The energy ranges of the electron and the positron can be treated from 1 keV for low Z material and from tens of keV to several thousand GeV for high Z material, and the photon can be treated from 1 keV to several thousand GeV.

Moreover, when electrons pass in the material, the energy is dissipated through the ionization of the material and the propagation direction is shifted by multiple scattering. In the process, X-rays are radiated via bremsstrahlung, photoelectric effect, Compton scattering, and the electron pair creation, etc., resulting in the electromagnetic cascade shower happens. The types of Fredholm transportation equation and the Monte-Carlo method are used as a basis for this electromagnetic cascade shower. The particle translocation is as follows : (1) Set the initial particle location, energy, and weight, (2) Determine the free path of the particle to the next collision point, (3) Calculate the weight on the particle with the next collision point, (4) Settle the scattering angle according to energy and incident angle in the next collision point. The process ends if the energy is below the cut-off within the range of the object otherwise the calculation goes back to step 2. In the calculation, the step

author's e-mail: okabayashi-a@ile.osaka-u.ac.jp

size is not decided discretely but is taken as a sampling random hinge [3, 7, 8, 9]. Physical mechanisms of the collisional processes such as stopping power, bremsstrahlung, Møller scattering, BhaBha scattering, positron annihilation, electron impact ionization, multiple scattering, electron pair creation, Compton scattering, Rayleigh scattering, photoelectric absorption, and Auger electrons can be treated in EGS5 for the particle transportation.

## 2. Simulation Condition

In EGS5 simulation, required are the conditions of the material composition, geometry, incident particle, and the physical mechanism of object substance. In our calculations, the superdense material geometry is taken from the high density plasma core at the integrated FI experiment [4] at Institute of Laser Engineering, Osaka University. The input electron energy distribution is used from the fitting on the experimental data of magnet electron spectrometer (ESM) [5, 6].

### 2.1 Material Condition

The plasma electron density profile of the superdense matter is fitted by a suitable Gaussian function onto the data point [4, 10]. The fitting function is shown as follows.

$$f(z) = 6.995 \cdot \exp \left\{ - \left( \frac{z[\text{cm}]}{0.0046} \right)^2 \right\} - 5.346. \quad (1)$$

Since it is difficult to define the density and the material composition by a continuous function on the programming material composition data in EGS5 simulations, a certain interval is given to divide the core sphere (radius  $\sim 24\mu\text{m}$ ) into 9 layers where the highest density is set at the center and each electron density districts [ $10^{-4}\text{cm}$ ] corresponding to the distance  $z$  from the center : 5.00, 6.80, 10.0, 12.3, 15.0, 16.6, 20.5, 21.8, 24.1, as shown in the function of the following equation (for the unit, [ $10^{25}/\text{cm}^3$ ]). In these regions, the average of mass density is  $53\text{ g}/\text{cm}^3$ . The substance is made of  $\text{C}_8\text{D}_8$  to reconstruct CD plasma.

### 2.2 Incident Particle Condition

Regarding to the incident particle condition, it is necessary to approximate the energy spectrum of fast electrons with a relativistic Maxwellian that fits well with the ESM experimental data [5]. The electron numbers in the high-energy part of this distribution is quite less than the low-energy part, so that the distribution of high energy electrons is not so important on the fitting (only less than 10 MeV fast electrons are well fitted to the approximation) [Fig. 1(a)].

In actual condition the laser ray enters into the material with a variety of angle of incidence angles via small F-number focusing optics. Therefore, the electron spatial distribution was appropriately given

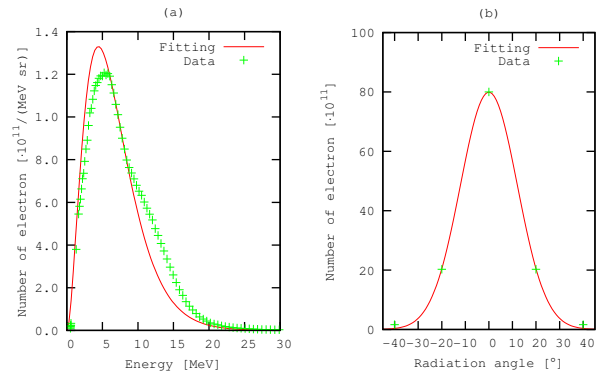


Fig. 1 (a) Energy spectrum of fast electrons by relativistic Maxwellian. and (b) Electron number about the incident angle in this simulation

by Gaussian distribution as centering the laser directions ( $0^\circ$ ) with about  $\pm 20^\circ$  dispersions ( $40^\circ$  FWHM) [Fig. 1(b)].

### 2.3 Physics Condition

Multiple scattering, bremsstrahlung, Møller scattering, and electron pair creation, Compton scattering, Rayleigh scattering, and photoelectric absorption are considered as physical mechanisms in the software package. However, neither BhaBha scattering, positron annihilation, nor electron impact ionization are considered from the energy range in this simulation for the reasons that the effects are almost negligible. Moreover, the equilibrium plasma that ionized completely has been assumed, so that the optional definitions [3] such as Auger electron, polarized lights of the secondary photon, and Compton profiles are not taken into consideration.

### 2.4 Region Condition

To evaluate the local energy deposition on a superdense matter, the mesh was adapted to the sphere with grid lines which cut a circumscribed cube into  $4 \times 4 \times 4$ . In the result, the sphere is subdivided to 296 regions as the logical product [3] of the sphere in the code.

## 3. Results and Discussions

At first we check whether the incident electrons are correctly generated in the calculation. The output average energy of the spectrum was 6.65 MeV when the no plasma is presented. The energy spectrum uses the approximate function by a relativistic Maxwellian and the average energy is calculated with  $3T_e$  by argument  $1/T_e$  about the electron temperature of the spectrum. The fitting curve we used is  $T_e = 1/0.4512$ , resulting in  $3T_e \doteq 6.648$ , in agreement with the output value above. This indicates that the incident particles were handled correctly in the calculation.

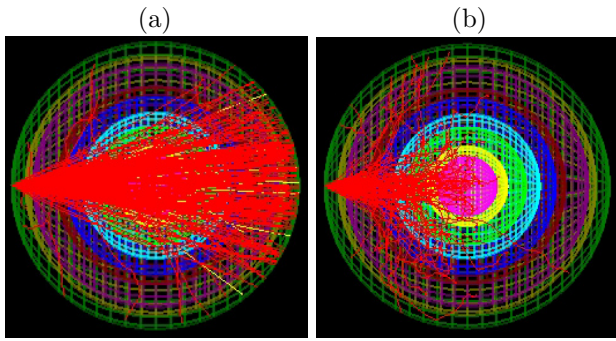


Fig. 2 (a) Particle track data in the case that incident electron spectrum is relativistic Maxwellian, and (b) mono energy of 0.5 MeV. The diameter of the most outside sphere is 0.00482 cm.

The track data of electrons is shown in Fig. 2(a). Around the incidence axis of laser, the high-energy electron easily passes through the superdense matter. On the other hand the low-energy electron is stopped because of multiple scattering by the collision and apparently has been absorbed. It is clear that the energy deposition rate of the low-energy electron ( $\leq 1$  MeV) is significant. In the calculation result, the whole energy deposition to the superdense matter was about  $0.384 \text{ MeV} \times \text{electron number}$  (10 millions).

It is interesting to consider energy deposition by mono energy electrons at the low-energy range without changing other conditions for this simulation. The calculation results are shown in Table 1 and the track data in the case of the 0.5 MeV energy is shown in Fig. 2(b). The energy deposition gives 80-100 % of the energy of the electron to the vicinity of 0.5 MeV, 50-70 % for 0.7-1 MeV, and the energy deposition decreases to 0.38 MeV gradually when incident energy is over 3 MeV. Therefore, it is clear that the energy deposition to the core can increase if fast electrons of which energy is around 1 MeV can be enhanced.

Finally we calculate the electron temperature from the energy deposition in each region using a relativistic Maxwellian as the electron spectrum. In the energy deposition processes, the energy was also consumed for creation of secondary particles such as X-ray. However, the energy deposition by photons is usually smaller than the thermal energy, so that all of energy deposition  $\epsilon$  was used for heating and then calculated the temperature from  $\epsilon = (3/2)T$ . For the simplicity, ion temperature  $T_i$  is assumed to be same with electron temperature  $T_e$  ( $T_e = T/2$ ). The laser beam (equivalent to the electron beam) irradiates from left to right in the geometry. The energy deposition calculated in each region is divided by the volume and the electron density of the region. The value was normalized by the initial energy of fast electrons = 24 J (the laser energy = 60 J and the conversion efficiency 40 %). As the result, the maximum electron temperature

Table 1. Energy deposition in the case that incident electron spectrum is mono-energetic.

incident energy [MeV]	energy deposition [MeV]
0.1	0.096
0.3	0.279
0.5	0.434
0.7	0.515
1.0	0.450
3.0	0.388
5.0	0.381
7.0	0.380
10.0	0.379

in all regions becomes 50 eV at the core center in the case of energy spectrum by Relativistic Maxwellian ( $T_e = 2.216 \text{ MeV}$ ).

In the recent experiment [4] at the same conditions, the core temperature is 120 eV ( $\pm 20\%$ ) from the number of thermonuclear neutrons when 60 J additional laser light was injected. In the simulation, the calculated temperature of 50 eV at the core center is less than 120 eV ( $\pm 20\%$ ). This may be reasonable by considering that the calculation includes only collisional processes.

Giving the temperature distribution smoothly, the calculated temperatures are normalized by multiplying the each divided cross section by the electron temperature value in each region. However, it is difficult to visualize the distribution of temperature in an automatic operation according to the numerical value since these values are calculated each complicated region, not the point. Therefore, it is normalized by the highest value in the whole region and colored with ten sub-stages manually as shown in Fig. 3.

According to distribution of temperature on Fig. 3, it can be confirmed that the electron temperatures are heated to a higher temperature along the laser axis, and are not significant on the low density region. Moreover, the heated temperature increases from the direction of the incidence to the core gradually.

However, in some places, there is a jump between adjacent regions on the electron temperature. This is due to the following artificial reason. At first the rough and non-uniformly mesh size of sliced regions is set in space otherwise the calculation will be very complex. Second, if the region size is larger compared with the spread of the electron as shown in figure 1(b), the averaged electron temperature of the region becomes unnatural although the part where the electron temperature is high and low exists in one region. Thirdly, when the region thickness is very thin, the random hinge that controls step size of EGS5 gives the energy deposition in the previous area that should be

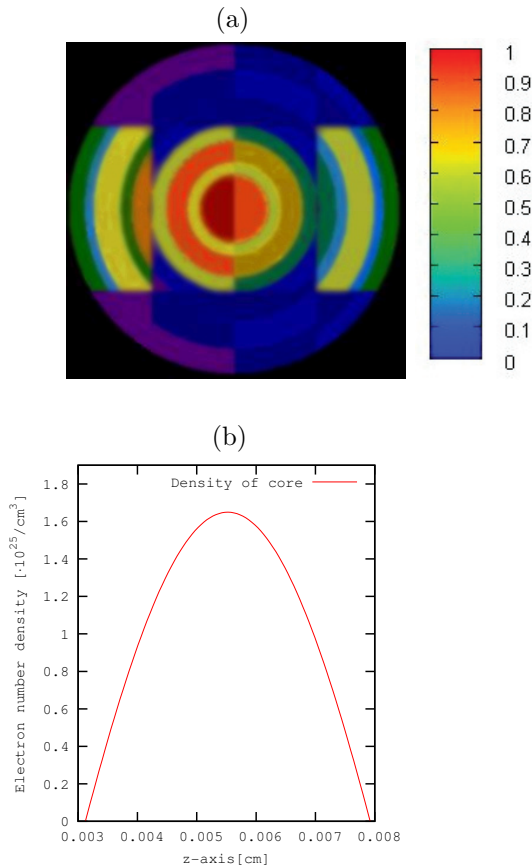


Fig. 3 (a) Distribution of normalized temperature and (b) the density profile for the superdense matter. The radius of the most outside circle is 0.00241 cm.

given into the following area, so that the error margin in each region extends intensively in one step point where the energy deposition between steps was decided by random numbers. Finally, there are some regions whose sizes are too small for the fast electrons to pass through.

#### 4. Conclusion

When the electron with mono-energy of 0.1-0.5 MeV is incident in the superdense matter created by high energy implosion laser beams, the most of the electron energy is absorbed in the corona plasma compared with much higher energy electrons. Therefore when the electron number at the energy of 0.5-1 MeV can be enhanced in the ultra-intense laser plasma interactions, we expect the average energy deposition becomes more than 0.38 MeV, showing a possibility that the efficient energy absorption at the core. Moreover, even if only the collisional process is considered in the physical process of energy deposition onto the superdense matter, it is gradually heated from a region near direction of the incidence of the electron, and the maximum temperature is obtained at the core up to 50 eV (incident laser energy : 60 J). This is less than half

of the experimentally estimated temperature. However these results exhibit that the collisional process is significantly important to heating of the core plasma.

In integrated fast ignition experiment planned in the future, it is expected that the laser energy will be about 160 times that of this simulation. Therefore, the electron temperature at the core could reach about 8 keV, based on our calculation. It is very interesting see the outcome of such fast ignition experiments in the near future.

#### - Reference -

- [1] M. Tabak, J. Hammer, M. E. Glinsky, W. L. Kruer, S. C. Wilks, J. Woodworth, E. M. Campbell, M. D. Perry, and R. J. Mason, *Ignition and high gain with ultrapowerful lasers*. Phys. Plasmas **1**, 1626 (1994).
- [2] A. J. Kemp, Y. Sentoku, V. Sotnikov, and S. C. Wilks, *Collisional Relaxation of Superthermal Electrons Generated by Relativistic Laser Pulses in Dense Plasma*. Phys. Rev. Lett. **97**, 235001 (2006).
- [3] KEK, Stanford Linear Accelerator Center, the University of Michigan teams, *SLAC-R-730*, (2007).
- [4] R. Kodama, P. A. Norreys, K. Mima, A. E. Dangor, R. G. Evans, H. Fujita, Y. Kitagawa, K. Krushelnick, T. Miyakoshi, N. Miyanaga, T. Norimatsu, S. J. Rose, T. Shozaki, K. Shigemori, A. Sunahara, M. Tampo, K. A. Tanaka, Y. Toyama, T. Yamanaka, and M. Zepf, *Fast heating of ultrahigh-density plasma as a step towards laser fusion ignition*. Nature, **412**, 798, (2001).
- [5] T. Yabuuchi, K. Adumi, H. Habara, R. Kodama, K. Kondo, T. Tanimoto, K. A. Tanaka, Y. Sentoku, T. Matsuoka, Z. L. Chen, M. Tampo, A. L. Lei, and K. Mima, *On the behavior of ultraintense laser produced hot electrons in self-excited fields*. Physics of Plasmas, **14**, 040706, (2007).
- [6] K. A. Tanaka, T. Yabuuchi, T. Sato, R. Kodama, Y. Kitagawa, T. Takahashi, T. Ikeda, Y. Honda, and S. Okuda, *Calibration of imaging plate for high energy electron spectrometer*. Rev. Sci. Instrum, **76**, 013507, (2005).
- [7] H. G. Paretzke, *Radiation Track Theory in Kinetics of Nonhomogeneous Processes*, G. R. Freeman ed., (Wiley Interscience, New York, 1980).
- [8] S. A. Goudsmit and J. L. Saunderson, *Multiple Scattering of Electrons*. Phys. Rev. **57**, 24 (1940).
- [9] C. Garban-Labaune, E. Fabre, C. E. Max, R. Fabbro, F. Amiranoff, J. Virmont, M. Weinfeld, and A. Michard, *Effect of Laser Wavelength and Pulse Duration on Laser-Light Absorption and Back Reflection*. Phys. Rev. Lett. **48**, 1018 (1982).
- [10] R. B. Campbell, R. Kodama, T. A. Mehlhorn, K. A. Tanaka, and D. R. Welch, *Simulation of Heating-Compressed Fast-Ignition Cores by Petawatt Laser-Generated Electrons*. Phys. Rev. Lett. **94**, 055001, (2005).